JACS
JOURNAL OF THE AMERICAN CHEMICAL SOCIETY

pubs.acs.org/JACS

Communication

Solid-State Pathway Control via Reaction-Directing Heteroatoms: Ordered Pyridazine Nanothreads through Selective Cycloaddition

Samuel G. Dunning,* Li Zhu, Bo Chen, Stella Chariton, Vitali B. Prakapenka, Maddury Somayazulu, and Timothy A. Strobel*

Cite This: https://doi.org/10.1021/jacs.1c12143

Read Online

ACCESS | Metrics & More | Article Recommendations | Supporting Information

ABSTRACT: Nanothreads are one-dimensional nanomaterials composed of a primarily sp^3 hydrocarbon backbone, typically formed through the compression of small molecules to high pressures. Although nanothreads have been synthesized from a range of precursors, controlling reaction pathways to produce atomically precise materials remains a difficult challenge. Here, we show how heteroatoms within precursors can serve as "thread-directing" groups by selecting for specific cycloaddition reaction pathways. By using a less-reactive diazine group within a six-membered aromatic ring, we successfully predict and synthesize the first carbon nanothread material derived from pyridazine (1,2-diazine, $C_4H_4N_2$). Compared with previous nanothreads, the synthesized polypyridazine, shows a predominantly uniform chemical structure with exceptional long-range order, allowing for structural characterization using vibrational spectroscopy and X-ray diffraction. The results demonstrate how thread-directing groups can be used for reaction pathway control and the formation of chemically precise nanothreads with a high degree of structural order.

In 2015, it was found that the slow room-temperature compression of benzene produced nanothreads—crystalline, one-dimensional polymers composed of sp^3 diamondoid bonds.[1] Whereas previous high-pressure reactions of small molecules resulted in amorphous products,[2−11] the discovery of ordered nanothreads suggests the existence of rational design principles for the controlled formation of crystalline extended solids at high pressure. These diamond-like materials that border nanotubes and polymers are predicted to possess enhanced mechanical, thermal, and chemical stability, making them ideal candidates for a diverse range of applications.[12−16]

Several design principles have been established to assess the likelihood that a precursor molecule will form ordered nanothreads with minimal atomic displacement. For aromatic precursors, π-stacking interactions between neighbors play an important role in reaction pathway selectivity as short inter-ring distances along stacks can limit potential reaction pathways. Precursors with nonparallel/significantly displaced π-stacks typically require slow (GPa/h) anisotropic compression to produce crystalline products.[1,17,18] Conversely, precursors composed of parallel−displaced/sandwich-like π-stacks were demonstrated to produce ordered nanothreads via rapid compression, even under quasi-hydrostatic conditions.[19−22] Stacking overlap can be quantified by using factors such as the distance between ring centroids (d_c), ring planes (d_p), and the slippage angle between ring centroids (ϕ).[19]

Heteroatom incorporation into thread-forming precursors provides additional opportunities to tune synthetic pathways and tailor nanothread properties for specific advanced applications.[23−25] This approach may also provide a level of synthetic control that is currently unavailable for purely carbon-based systems. For example, in aromatic hydrocarbons each carbon−carbon bond is potentially capable of participating in [4 + 2] cycloaddition, providing a number of competing pathways and a distribution of products.[26−28] In comparison, nanothreads derived from furan[29] and thiophene[30] indicate enhanced structural order due, in large part, to their localized bonding, which limits potential reaction pathways to [4 + 2] cycloaddition between the carbon atoms in the ring, confirmed by advanced NMR studies of furan nanothreads.[31] If such predictable reactivity could be generalized to more complex nanothread systems, it would represent a major advancement for controlled solid-state synthesis and enable the *a priori* prediction of polymerized nanothread structures from their precursor structures alone.

While the use of heteroatoms as thread-directing groups has not yet been explicitly investigated in the hypothesis-driven synthesis of a target product, previous reports of nanothreads synthesized from N-bearing precursors indicate that nitrogen heteroatom substitution may be used to guide nanothread formation. ^{13}C NMR of pyridine-derived nanothreads determined that N═CH bonds are most likely to persist in degree 4 products.[18] In addition, azobenzene-derived double-core nanothreads show that the azo (N═N) group persists even after compression to 20 GPa.[32,33] These studies indicate that bonds containing nitrogen may be less reactive in comparison to analogous carbon−carbon bonds. Therefore, if nitrogen is incorporated strategically within the precursor with respect to molecular packing, it may be able to direct

Received: November 17, 2021

nanothread formation toward atomically precise chemical products with long-range order.

On the basis of these factors, we compiled potential thread-forming aromatic precursors that crystallize with significant π-stacking interactions and also incorporate nitrogen heteroatoms so as to direct the in-stack reaction pathway. Pyridazine (1,2-diazine, $C_4H_4N_2$) shows near-sandwich-type π-stacking[34] (i.e., d_c < ∼4 Å, Φ < ∼25°, Figure 1A,B), suggesting it is an excellent candidate to undergo pressure-induced polymerization down the stacking axis.[19] Additionally, pyridazine possesses a much longer nitrogen−nitrogen bond (N1−N2 = 1.431 Å) and shorter carbon−nitrogen bonds (avg = 1.322 Å) relative to other comparable heterocycles,[34−38] suggesting the respective bonds have more single- and double-bond character than truly resonant systems. With this in mind, we propose that compressed pyridazine will undergo a direct topochemical-like, nanothread-forming reaction in which the nitrogen atoms serve as a thread-directing group by restricting polymerization to a single, carbon-exclusive [4 + 2] cycloaddition down the stacking axis, in agreement with previous theoretical studies.[39] On the basis of the molecular crystal structure, we hypothesize nanothreads with azo bonds aligned on one side (*syn* conformation), producing a distinct, ordered chemical structure with an anisotropic azimuthal cross section.

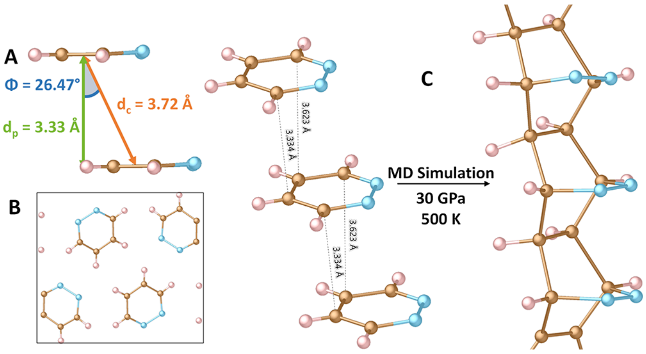

Figure 1. (A) Structure of pyridazine-I showing local π-stacking at 0.61 GPa. (B) π-Stacking of pyridazine along the *a*-axis. (C) (left) Close-contact [4 + 2] cycloaddition pathway within pyridazine; (right) *syn*-NN nanothread structure observed in first-principles molecular dynamics (MD) simulation at 500 K and 30 GPa.

As an initial step to test the hypothesis of controlled polymerization in compressed pyridazine, energy barrier (Figure S1) and first-principles molecular dynamics (MD) simulations were conducted for crystalline pyridazine at 30 GPa and 500 K. After 230 fs (Figure S2), a spontaneous reaction initiates between carbons in adjacent rings via [4 + 2] cycloaddition, producing the polymerized product shown in Figure 1C. This product represents the closest-contact reaction pathway. This degree-4 nanothread consists of a sp^3-bonded carbon backbone with a pendant *syn*-N═N group, resulting from exclusive carbon reactions down the stacking axis. The observation of spontaneous polymerization at moderate PT conditions suggests an energetically favorable reaction pathway and provides initial validation of pyridazine as a viable precursor candidate for controlled, heteroatom-directed synthesis. The *syn*-NN structure is also favorable based on barrier and reaction energy considerations.

To validate polymerization experimentally, liquid pyridazine was loaded into diamond anvil cells (DAC) and compressed to 32 GPa. Liquid pyridazine solidified at ∼0.2 GPa, and *in situ* X-ray diffraction (XRD) patterns were readily indexed to the previously reported monoclinic structure.[34] Upon solidification, crystals exhibit strong preferred orientation, before exhibiting more powder-like character when broken up at higher pressures (Figure S3). Upon compression, Bragg peaks monotonically shift to higher angles reflecting contraction of the unit cell. Minor peak splitting was observed above 9.5 GPa, possibly indicative of a subtle polymorphic (molecular) phase transition (Figure 2A). Above 13 GPa new strong peaks appear at low and high angles, and the sample takes on an orange hue indicative of reaction onset in agreement with XRD (Figure 2B). Most notably, the emergence of a new 6-fold diffraction pattern indicates that this chemical transformation is consistent with nanothread formation (Figures S3−S7), and the relative

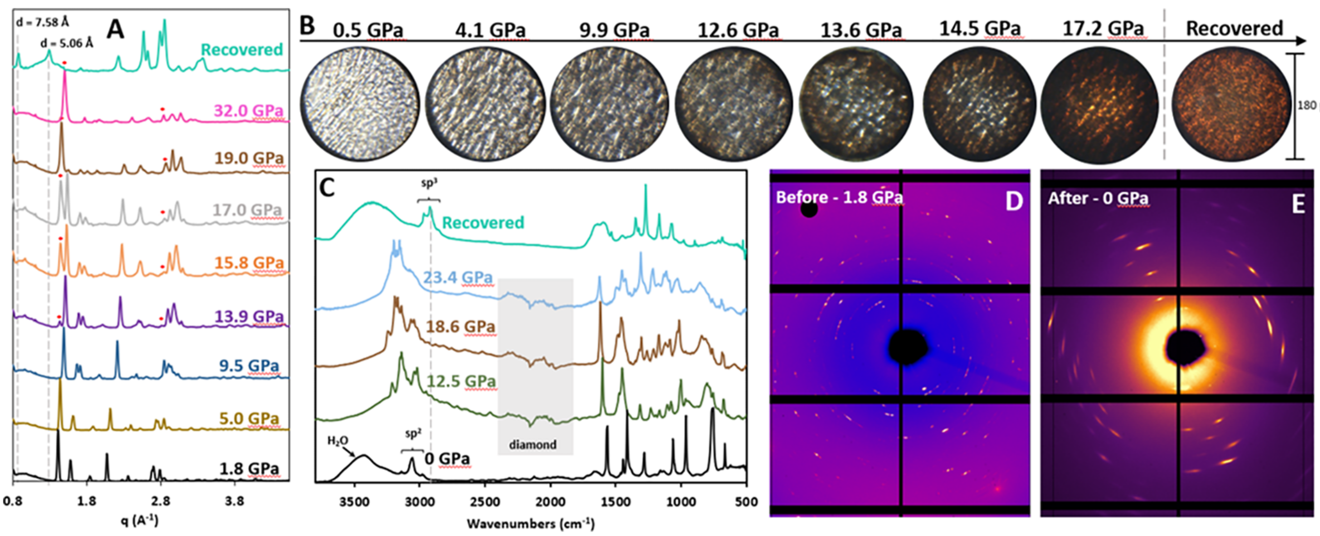

Figure 2. (A) *In situ* XRD patterns for 1,2-diazine, asterisks show new peaks during compression. (B) Micrographs of 1,2-diazine during compression (transmitted light). (C) FTIR absorbance spectra of 1,2-diazine with pressure. The gray box indicates artifacts from the diamond anvils. The broad band ca. 3400 cm^{-1} indicates the presence of absorbed H_2O. (D, E) 2D XRD patterns for 1,2-diazine before (1.8 GPa) and after polymerization (compressed to 32 GPa and recovered to ambient pressure).

https://doi.org/10.1021/jacs.1c12143
J. Am. Chem. Soc. XXXX, XXX, XXX−XXX

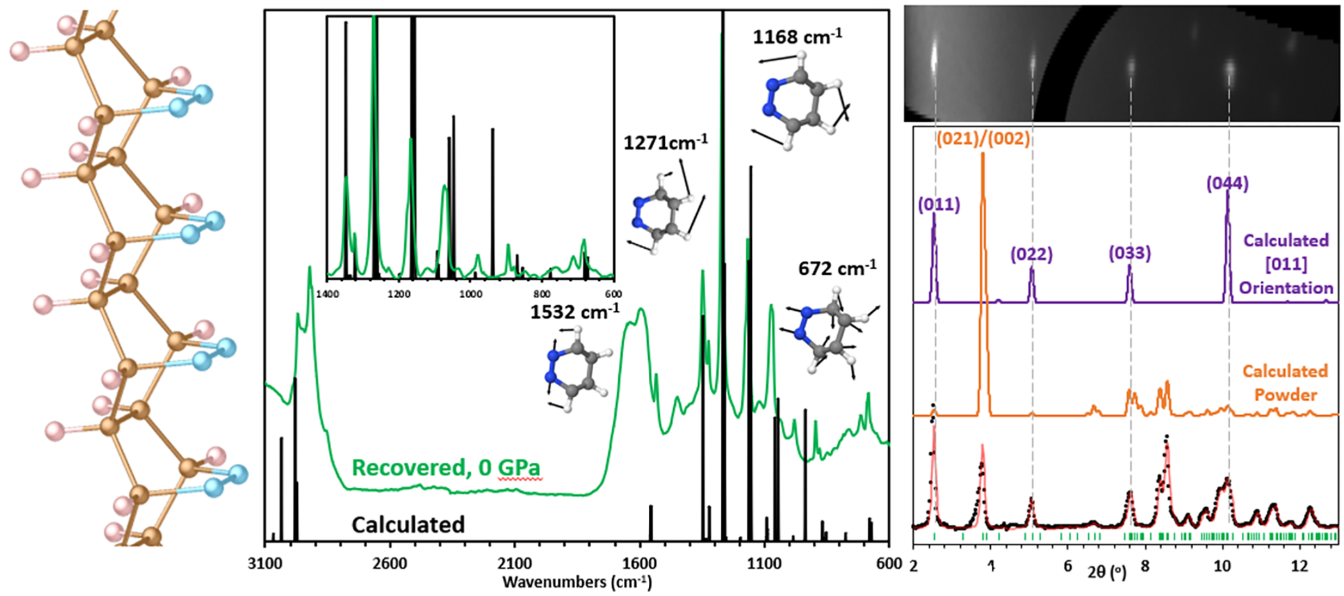

Figure 3. (left) Structure of the *syn*-NN polypyridazine nanothread. (center) Comparison of the experimental polypyridazine (green) and calculated *syn*-NN (black) IR spectra at 1 atm. The calculated spectrum is represented by Gaussian peaks with an arbitrary width. Inset: background-corrected spectrum between 600 and 1400 cm^{-1}. (right) XRD pattern of oriented polypyridazine at 1 atm (black points) with Le Bail refinement (red), λ = 0.3344 Å. Patterns for the *syn*-NN structure simulated by using refined cell parameters (orange) and with crystallites oriented in the [011] direction (purple) are shown for comparison. Top: experimental 2D XRD data showing intensity of spots associated with the (0, k, l = k) series.

shifts of the (021) and (002) Bragg peaks reflect nanothread formation from the pyridazine molecular geometry (see the Supporting Information). These new peaks become more intense with increasing pressure, while precursor peaks disappear completely above ca. 19 GPa. The new diffraction peaks persist when the DAC is opened to ambient condiions (Figures 2D,E), which indicates the formation of an extended crystalline polymer (liquid pyridazine evaporates at ambient conditions).

In situ vibrational spectra obtained during compression are consistent with the XRD results (Figure 2C and Figure S10). It should be noted that all samples contained some amount of absorbed H_2O (Supporting Information). Above 8 GPa, two new peaks in the FTIR spectrum emerge at ca. 962 and 1174 cm^{-1}, and the Raman spectrum shows splitting of peaks ca. 206 and 3104 cm^{-1} (Figures S15−S17), confirming a subtle polymorphic phase transition. This transition is reversible, and the starting FTIR spectrum is recovered upon decompression (Figure S14). Although we cannot solve the structure of this new molecular phase, it does not appear to involve a significant structural rearrangement based on the subtle spectral and diffraction changes. An irreversible chemical transformation occurs above 13 GPa, notably indicated by the emergence of new peaks in the sp^3 C−H stretching region in the FTIR and Raman spectra (ca. 3116 cm^{-1} at 13 GPa, Supporting Information), the onset of a color change which causes an increase in the fluorescence background in Raman spectra (Figures S15−S18), and the splitting of the sp^2 C−H stretching peak. The formation of sp^3 carbon is fully consistent with the nanothread-forming [4 + 2] cycloaddition reaction observed in MD simulations.

Recovered samples, hereafter termed polypyridazine, remain an orange translucent solid, similar to previously described carbon nitride nanothreads.[18,30] PXRD patterns of polypyridazine show distinct differences to that of molecular pyridazine, indicating that the recovered product possesses new structural packing. Compared with previous nanothreads such as benzene or pyridine, which show broad/weak diffraction below d = 5.6 Å due to considerable intrathread disorder,[1,17,40] polypyridazine exhibits crystalline diffraction to d-spacings below 1.2 Å, indicating precise atomic ordering of individual threads. This intense high-angle diffraction suggests polypyridazine may approach "perfect" chemical ordering similar to furan nanothreads, a fraction of which were determined to be "perfect" by solid-state ^{13}C NMR.[31]

The FTIR spectrum of polypyridazine exhibits extremely well-defined absorption features, further indicating a high degree of structural order. These absorption bands are notably sharp in comparison to previously reported carbon nitride nanothreads and amorphous carbon nitride films.[40−43] Following evidence for controlled polymerization via MD simulations and diffraction/spectroscopy, we optimized a packed *syn*-NN nanothread model using DFT for quantitative comparisons with experimental observables. A comparison of the experimental and calculated FTIR spectra for the *syn*-NN structure shows that the two are an exceptional match (Figure 3) and for the first time allows for the complete assignment of the IR spectrum of a nanothread material. The Supporting Information details peak assignments for polypridazine (Table S2) and any defects or impurities such as absorbed H_2O present (Figures S11−S13). Notably, the intense peaks at ca. 2968 and 2924 cm^{-1} can be assigned to sp^3 C−H stretching vibrations, consistent with previously reported nanothreads. The peak ca. 1532 cm^{-1} is clearly attributed to N=N stretching, in good agreement with molecular *cis*-diazine systems.[44−46] Notably, the N=N bond distance is smaller than that in molecular pyridazine (1.25 Å vs 1.43 Å), and this higher-frequency stretch is diagnostic of the *syn*-NN polymer due to the [4 + 2] reaction of the carbon atoms and the formation of a N=N double bond.

https://doi.org/10.1021/jacs.1c12143
J. Am. Chem. Soc. XXXX, XXX, XXX−XXX

The simulated XRD pattern for the DFT-optimized *syn*-NN structure also shows good agreement with experimental data (Figure 3). Recovered samples always showed the crystallographic preferred orientation; however, by averaging multiple diffraction patterns, we were able to improve powder averaging statistics and index a monoclinic lattice. The ability to index to a three-dimensional lattice establishes enhanced structural ordering of the product compared with other nanothread materials. Refinement of the experimental unit cell at room temperature using the Le Bail method gives the lattice parameters a = 2.568(4) Å, b = 9.88(2) Å, c = 11.78(2) Å, and β = 90.51(3)°, which compare favorably with the DFT-optimized (0 K) *syn*-NN structure (a = 2.59 Å, b = 9.75 Å, c = 11.53 Å, and β = 90.01°; space group = $P2_1$). Notably, the length of a is significantly smaller than the starting molecular crystal (~3.7 Å at 0.6 GPa) due to polymerization down the stacking axis. Changes in the b and c dimensions reflect changes in geometry and hydrogen bonding caused by nanothread formation (Figure S7). While several other polypyridazine nanothread structures are possible, only the degree-4, *syn*-NN model can describe both the experimental XRD and FTIR data (see the Supporting Information).

Finally, thermal decomposition experiments were performed to confirm the structure of polypyridazine. If the *syn*-NN structure is correct, it should be possible to postsynthetically remove the azo groups as N_2 gas via thermal decomposition.[47−50] A sample of polypyridazine was loaded into an optical cell and monitored by *in situ* FTIR measurements (Figure 4). After heating the sample at 250 °C for 72 h a new,

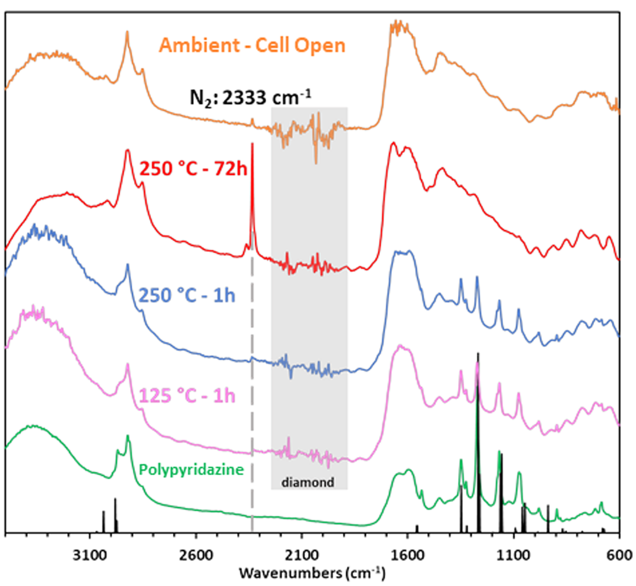

Figure 4. FTIR spectra of polypyridazine under ambient conditions (green); after heating at different conditions. The calculated spectrum is shown in black.

sharp absorption peak appears at ca. 2333 cm^{-1}, corresponding to physisorbed N_2 (cf. 2331 cm^{-1}).[51,52] All thread-related peaks below 1600 cm^{-1} disappear with only the sp^3 nature of carbon product remaining clear via C−H vibrations near 2900 cm^{-1}. Raman measurements collected under the same conditions show a notable decrease in fluorescence (see Figure S19), consistent with the loss of nitrogen from the nanothread.[18] These data confirm the pendant N═N nature of the nanothread polymer.

The level of structural control over nanothread forming reactions shown in the synthesis of polypyridazine is encouraging for the design of future nanothread systems. This work indicates that careful heteroatom incorporation can be used to limit the number of potential reaction pathways and obtain highly ordered nanothread products. Further investigation of other heterocyclic ring systems is needed to understand the scope of this synthetic strategy.

■ ASSOCIATED CONTENT

Supporting Information

The Supporting Information is available free of charge at https://pubs.acs.org/doi/10.1021/jacs.1c12143.

Diffraction and spectroscopic data as well as computational models (PDF)
File S1 (ZIP)
File S2 (ZIP)

■ AUTHOR INFORMATION

Corresponding Authors

Samuel G. Dunning − *Earth and Planets Laboratory, Carnegie Institution for Science, Washington, D.C. 20015, United States*; orcid.org/0000-0003-1011-8339; Email: sdunning@carnegiescience.edu

Timothy A. Strobel − *Earth and Planets Laboratory, Carnegie Institution for Science, Washington, D.C. 20015, United States*; orcid.org/0000-0003-0338-4380; Email: tstrobel@carnegiescience.edu

Authors

Li Zhu − *Earth and Planets Laboratory, Carnegie Institution for Science, Washington, D.C. 20015, United States*; orcid.org/0000-0001-8588-9379

Bo Chen − *Donostia International Physics Center, 20018 Donostia-San Sebastian, Spain; IKERBASQUE - Basque Foundation for Science, 48009 Bilbao, Spain*; orcid.org/0000-0002-5084-1321

Stella Chariton − *Center for Advanced Radiation Sources, The University of Chicago, Chicago, Illinois 60637, United States*; orcid.org/0000-0001-5522-0498

Vitali B. Prakapenka − *Center for Advanced Radiation Sources, The University of Chicago, Chicago, Illinois 60637, United States*

Maddury Somayazulu − *HPCAT, X-ray Science Division, Argonne National Laboratory, Lemont, Illinois 60439, United States*; orcid.org/0000-0001-5508-211X

Complete contact information is available at: https://pubs.acs.org/10.1021/jacs.1c12143

Funding

The authors acknowledge support from the U.S. Army Research Office under Grant W911NF-17-1-0604.

Notes

The authors declare no competing financial interest.

■ ACKNOWLEDGMENTS

The authors thank Dr. Thomas Shiell for his assistance in XRD data collection. Portions of this work were performed at GeoSoilEnviroCARS (The University of Chicago, Sector 13) and HPCAT (Sector 16), Advanced Photon Source (APS), Argonne National Laboratory. GeoSoilEnviroCARS is supported by the National Science Foundation - Earth Sciences

(EAR-1634415) and Department of Energy - GeoSciences (DE-FG02-94ER14466). HPCAT operations were supported by DOE-NNSA's Office of Experimental Sciences. This research used resources of the Advanced Photon Source, a U.S. Department of Energy (DOE) Office of Science User Facility operated for the DOE Office of Science by Argonne National Laboratory under Contract DE-AC02- 06CH11357.

■ ABBREVIATIONS

GPa, gigapascals; d_c, distance between ring centroids; d_p, distance between parallel ring planes; ϕ, slippage angle between rings; fs, femtoseconds; P, T, pressure and temperature; syn-NN, structure in which each N═N bond is oriented along the same side of the nanothread; anti-NN, structure in which N═N bonds are oriented along alternating sides of the nanothread; PXRD, powder X-ray diffraction; FTIR, Fourier-transform infrared spectroscopy; DAC, diamond anvil cell; NMR, nuclear magnetic resonance.

■ REFERENCES

(1) Fitzgibbons, T. C.; Guthrie, M.; Xu, E. S.; Crespi, V. H.; Davidowski, S. K.; Cody, G. D.; Alem, N.; Badding, J. V. Benzene-derived carbon nanothreads. *Nat. Mater.* **2015**, *14* (1), 43−47.

(2) Pruzan, P.; Chervin, J. C.; Thiery, M. M.; Itie, J. P.; Besson, J. M.; Forgerit, J. P.; Revault, M. Transformation of Benzene to a Polymer After Static Pressurization to 30 GPa. *J. Chem. Phys.* **1990**, *92* (11), 6910−6915.

(3) Ciabini, L.; Santoro, M.; Gorelli, F. A.; Bini, R.; Schettino, V.; Raugei, S. Triggering dynamics of the high-pressure benzene amorphization. *Nat. Mater.* **2007**, *6* (1), 39−43.

(4) Citroni, M.; Bini, R.; Foggi, P.; Schettino, V. Role of excited electronic states in the high-pressure amorphization of benzene. *Proc. Natl. Acad. Sci. U. S. A.* **2008**, *105* (22), 7658−7663.

(5) Schettino, V.; Bini, R. Constraining molecules at the closest approach: chemistry at high pressure. *Chem. Soc. Rev.* **2007**, *36* (6), 869−880.

(6) Ward, M. D.; Huang, H. T.; Zhu, L.; Popov, D.; Strobel, T. A. High-Pressure Behavior of C2I2 and Polymerization to a Conductive Polymer. *J. Phys. Chem. C* **2019**, *123* (18), 11369−11377.

(7) Wang, Q. Q.; Gou, H. Y.; Zhu, L.; Huang, H. T.; Biswas, A.; Chaloux, B. L.; Epshteyn, A.; Yesinowski, J. P.; Liu, Z. X.; Cody, G.; Ma, M. D.; Zhao, Z. S.; Fei, Y. W.; Prescher, C.; Greenberg, E.; Prakapenka, V. B.; Strobel, T. A. Modifying Carbon Nitride through Extreme Phosphorus Substitution. *Acs Materials Letters* **2019**, *1* (1), 14−19.

(8) Keefer, D. W.; Gou, H. Y.; Wang, Q. Q.; Purdy, A.; Epshteyn, A.; Juhl, S. J.; Cody, G. D.; Badding, J.; Strobel, T. A. Tetracyanomethane under Pressure: Extended CN Polymers from Precursors with Built-in sp(3) Centers. *J. Phys. Chem. A* **2018**, *122* (11), 2858−2863.

(9) Gou, H.; Zhu, L.; Huang, H.-T.; Biswas, A.; Keefer, D. W.; Chaloux, B. L.; Prescher, C.; Yang, L.; Kim, D. Y.; Ward, M. D.; Lerach, J.; Wang, S.; Oganov, A. R.; Epshteyn, A.; Badding, J. V.; Strobel, T. A. From Linear Molecular Chains to Extended Polycyclic Networks: Polymerization of Dicyanoacetylene. *Chem. Mater.* **2017**, *29* (16), 6706−6718.

(10) Gou, H. Y.; Yonke, B. L.; Epshteyn, A.; Kim, D. Y.; Smith, J. S.; Strobel, T. A. Pressure-induced polymerization of P(CN)(3). *J. Chem. Phys.* **2015**, *142* (19), 194503.

(11) Keefer, D. W.; Gou, H.; Purdy, A. P.; Epshteyn, A.; Kim, D. Y.; Badding, J. V.; Strobel, T. A. Pressure-Induced Polymerization of LiN(CN)(2). *J. Phys. Chem. A* **2016**, *120* (47), 9370−9377.

(12) Zhan, H. F.; Zhang, G.; Tan, V. B. C.; Cheng, Y.; Bell, J. M.; Zhang, Y. W.; Gu, Y. T. From brittle to ductile: a structure dependent ductility of diamond nanothread. *Nanoscale* **2016**, *8* (21), 11177−11184.

(13) Roman, R. E.; Kwan, K.; Cranford, S. W. Mechanical Properties and Defect Sensitivity of Diamond Nanothreads. *Nano Lett.* **2015**, *15* (3), 1585−1590.

(14) Silveira, J.; Muniz, A. R. First-principles calculation of the mechanical properties of diamond nanothreads. *Carbon* **2017**, *113*, 260−265.

(15) Zhou, W. X.; Cheng, Y.; Chen, K. Q.; Xie, G. F.; Wang, T.; Zhang, G. Thermal Conductivity of Amorphous Materials. *Adv. Funct. Mater.* **2020**, *30* (8), 1903829.

(16) Zhu, T. S.; Ertekin, E. Phonons, Localization, and Thermal Conductivity of Diamond Nanothreads and Amorphous Graphene. *Nano Lett.* **2016**, *16* (8), 4763−4772.

(17) Li, X.; Baldini, M.; Wang, T.; Chen, B.; Xu, E.-s.; Vermilyea, B.; Crespi, V. H.; Hoffmann, R.; Molaison, J. J.; Tulk, C. A.; Guthrie, M.; Sinogeikin, S.; Badding, J. V. Mechanochemical Synthesis of Carbon Nanothread Single Crystals. *J. Am. Chem. Soc.* **2017**, *139* (45), 16343−16349.

(18) Li, X.; Wang, T.; Duan, P.; Baldini, M.; Huang, H. T.; Chen, B.; Juhl, S. J.; Koeplinger, D.; Crespi, V. H.; Schmidt-Rohr, K.; Hoffmann, R.; Alem, N.; Guthrie, M.; Zhang, X.; Badding, J. V. Carbon Nitride Nanothread Crystals Derived from Pyridine. *J. Am. Chem. Soc.* **2018**, *140* (15), 4969−4972.

(19) Tang, W. S.; Strobel, T. A. Evidence for Functionalized Carbon Nanothreads from pi-Stacked, para-Disubstituted Benzenes. *J. Phys. Chem. C* **2020**, *124* (45), 25062−25070.

(20) Gerthoffer, M. C.; Wu, S. K.; Chen, B.; Wang, T.; Huss, S.; Oburn, S. M.; Crespi, V. H.; Badding, J. V.; Elacqua, E. 'Sacrificial' supramolecular assembly and pressure-induced polymerization: toward sequence-defined functionalized nanothreads. *Chemical Science* **2020**, *11* (42), 11419−11424.

(21) Ward, M. D.; Tang, W. S.; Zhu, L.; Popov, D.; Cody, G. D.; Strobel, T. A. Controlled Single-Crystalline Polymerization of C10H8·C10F8 under Pressure. *Macromolecules* **2019**, *52* (20), 7557−7563.

(22) Friedrich, A.; Collings, I. E.; Dziubek, K. F.; Fanetti, S.; Radacki, K.; Ruiz-Fuertes, J.; Pellicer-Porres, J.; Hanfland, M.; Sieh, D.; Bini, R.; Clark, S. J.; Marder, T. B. Pressure-Induced Polymerization of Polycyclic Arene-Perfluoroarene Cocrystals: Single Crystal X-ray Diffraction Studies, Reaction Kinetics, and Design of Columnar Hydrofluorocarbons. *J. Am. Chem. Soc.* **2020**, *142* (44), 18907−18923.

(23) Zheng, Z. Q.; Zhan, H. F.; Nie, Y. H.; Xu, X.; Gu, Y. T. Role of Nitrogen on the Mechanical Properties of the Novel Carbon Nitride Nanothreads. *J. Phys. Chem. C* **2019**, *123* (47), 28977−28984.

(24) Demingos, P. G.; Muniz, A. R. Electronic and Mechanical Properties of Partially Saturated Carbon and Carbon Nitride Nanothreads. *J. Phys. Chem. C* **2019**, *123* (6), 3886−3891.

(25) Demingos, P. G.; Balzaretti, N. M.; Muniz, A. R. First-principles study of carbon nanothreads derived from five-membered heterocyclic rings: thiophene, furan and pyrrole. *Phys. Chem. Chem. Phys.* **2021**, *23* (3), 2055−2062.

(26) Xu, E. S.; Lammert, P. E.; Crespi, V. H. Systematic Enumeration of sp(3) Nanothreads. *Nano Lett.* **2015**, *15* (8), 5124−5130.

(27) Duan, K.; Li, Y. J.; Li, L.; Hu, Y. J.; Wang, X. L. Diamond nanothread based resonators: ultrahigh sensitivity and low dissipation. *Nanoscale* **2018**, *10* (17), 8058−8065.

(28) Demingos, P. G.; Muniz, A. R. Carbon nanothreads from polycyclic aromatic hydrocarbon molecules. *Carbon* **2018**, *140*, 644−652.

(29) Huss, S.; Wu, S. K.; Chen, B.; Wang, T.; Gerthoffer, M. C.; Ryan, D. J.; Smith, S. E.; Crespi, V. H.; Badding, J. V.; Elacqua, E. Scalable Synthesis of Crystalline One-Dimensional Carbon Nanothreads through Modest-Pressure Polymerization of Furan. *ACS Nano* **2021**, *15* (3), 4134−4143.

(30) Biswas, A.; Ward, M. D.; Wang, T.; Zhu, L.; Huang, H. T.; Badding, J. V.; Crespi, V. H.; Strobel, T. A. Evidence for Orientational Order in Nanothreads Derived from Thiophene. *J. Phys. Chem. Lett.* **2019**, *10* (22), 7164−7171.

https://doi.org/10.1021/jacs.1c12143
J. Am. Chem. Soc. XXXX, XXX, XXX−XXX

(31) Matsuura, B. S.; Huss, S.; Zheng, Z. X.; Yuan, S. C.; Wang, T.; Chen, B.; Badding, J. V.; Trauner, D.; Elacqua, E.; van Duin, A. C. T.; Crespi, V. H.; Schmidt-Rohr, K. Perfect and Defective C-13-Furan-Derived Nanothreads from ModestPressure Synthesis Analyzed by C-13 NMR. *J. Am. Chem. Soc.* **2021**, *143* (25), 9529−9542.

(32) Romi, S.; Fanetti, S.; Alabarse, F.; Mio, A. M.; Bini, R. Synthesis of double core chromophore-functionalized nanothreads by compressing azobenzene in a diamond anvil cell. *Chemical Science* **2021**, *12* (20), 7048−7057.

(33) Romi, S.; Fanetti, S.; Alabarse, F.; Bini, R. Structure-Reactivity Relationship in the High-Pressure Formation of Double-Core Carbon Nanothreads from Azobenzene Crystal. *J. Phys. Chem. C* **2021**, *125* (31), 17174−17182.

(34) Podsiadlo, M.; Jakobek, K.; Katrusiak, A. Density, freezing and molecular aggregation in pyridazine, pyridine and benzene. *CrystEngComm* **2010**, *12* (9), 2561−2567.

(35) Patyk, E.; Podsiadlo, M.; Katrusiak, A. CH···N Bonds and Dynamics in Isostructural Pyrimidine Polymorphs. *Cryst. Growth Des.* **2015**, *15* (8), 4039−4044.

(36) Patyk, E.; Podsiadlo, M.; Katrusiak, A. Discrete CH···N Bonded Patterns Modified by Temperature and Pressure in Four Pyrazine Polymorphs. *Cryst. Growth Des.* **2015**, *15* (12), 5670−5674.

(37) Prasad, S. M.; Rae, A. I. M.; Hewat, A. W.; Pawley, G. S. The Crystal-Structure of s-Triazine At 5 K. *Journal of Physics C-Solid State Physics* **1981**, *14* (31), L929−L931.

(38) Nelyubina, Y. V.; Korlyukov, A. A.; Lyssenko, K. A. Probing Weak Intermolecular Interactions by Using the Invariom Approach: A Comparative Study of s-Tetrazine. *Chem.—Eur. J.* **2014**, *20* (23), 6978−6984.

(39) Yang, Y. F.; Liang, Y.; Liu, F.; Houk, K. N. Diels-Alder Reactivities of Benzene, Pyridine, and Di-, Tri-, and Tetrazines: The Roles of Geometrical Distortions and Orbital Interactions. *J. Am. Chem. Soc.* **2016**, *138* (5), 1660−1667.

(40) Zhang, L. W.; Ji, W. M.; Liew, K. M. Mechanical properties of diamond nanothread reinforced polymer composites. *Carbon* **2018**, *132*, 232−240.

(41) Rodil, S. E.; Ferrari, A. C.; Robertson, J.; Milne, W. I. Raman and infrared modes of hydrogenated amorphous carbon nitride. *J. Appl. Phys.* **2001**, *89* (10), 5425−5430.

(42) Ferrari, A. C.; Rodil, S. E.; Robertson, J. Interpretation of infrared and Raman spectra of amorphous carbon nitrides. *Phys. Rev. B* **2003**, *67* (15), 155306.

(43) Citroni, M.; Fanetti, S.; Bazzicalupi, C.; Dziubek, K.; Pagliai, M.; Nobrega, M. M.; Mezouar, M.; Bini, R. Structural and Electronic Competing Mechanisms in the Formation of Amorphous Carbon Nitride by Compressing s-Triazine. *J. Phys. Chem. C* **2015**, *119* (51), 28560−28569.

(44) Zimmermann, F.; Lippert, T.; Beyer, C.; Stebani, J.; Nuyken, O.; Wokaun, A. N═N Vibrational Frequencies and Fragmentation Patterns of Substituted 1-Aryl-3,3-Dialkyl-Triazenes - Comparison With Other High-Nitrogen Compounds. *Appl. Spectrosc.* **1993**, *47* (7), 986−993.

(45) Ackermann, M. N.; Craig, N. C.; Isberg, R. R.; Lauter, D. M.; Macphail, R. A.; Young, W. G. cis-Dimethyldiazene. *J. Am. Chem. Soc.* **1977**, *99* (5), 1661−1663.

(46) Ackermann, M. N.; Craig, N. C.; Isberg, R. R.; Lauter, D. M.; Tacy, E. P. Vibrational-Spectra of cis-Dimethyldiazene-D0,-1,1,1-D3, and-D6. *J. Phys. Chem.* **1979**, *83* (9), 1190−1200.

(47) Nguyen, T.; Saleh, M. Thermal degradation of azobenzene dyes. *Results in Chemistry* **2020**, *2*, 100085.

(48) Engel, P. S.; Horsey, D. W.; Keys, D. E.; Nalepa, C. J.; Soltero, L. R. Photolysis of Reluctant Azoalkanes - Effect of Structure on Photochemical Loss of Nitrogen From 2,3-Diazabicyclo 2.2.2 oct-2-ene Derivatives. *J. Am. Chem. Soc.* **1983**, *105* (24), 7108−7114.

(49) Hore, N. R.; Russell, D. K. Radical pathways in the thermal decomposition of pyridine and diazines: a laser pyrolysis and semi-empirical study. *J. Chem. Soc.-Perkin Transactions* **1998**, *2* (2), 269−275.

(50) Dervan, P. B.; Santilli, D. S. Synthesis and Thermal-Decomposition of Cis-3,4,5,6-Tetrahydropyridazine-3,4-D2 - Relative Rates of Rotation, Cleavage, and Closure for Tetramethylene. *J. Am. Chem. Soc.* **1980**, *102* (11), 3863−3870.

(51) Herzberg, G. *Molecular Spectra and Molecular Structure: Spectra of Diatomic Molecules*; Van Nostrand: 1950.

(52) Gustafsson, K.; Karlberg, G. S.; Andersson, S. Infrared spectroscopy of physisorbed and chemisorbed N2 in the Pt(111)(3 × 3)N2 structure. *J. Chem. Phys.* **2007**, *127* (19), 194708.

https://doi.org/10.1021/jacs.1c12143
J. Am. Chem. Soc. XXXX, XXX, XXX−XXX